J Mol Model (2013) 19:673–688
DOI 10.1007/s00894-012-1590-1

ORIGINAL PAPER

Molecular dynamics analysis of a series of 22 potential farnesyltransferase substrates containing a CaaX-motif

Sérgio F. Sousa · João T. S. Coimbra · Diogo Paramos · Rita Pinto · Rodrigo S. Guimarães · Vitor Teixeira · Pedro A. Fernandes · Maria J. Ramos

Received: 16 July 2012 / Accepted: 29 August 2012 / Published online: 26 September 2012
© Springer-Verlag 2012

Abstract Protein farnesyltransferase (FTase) is an important target in many research fields, more markedly so in cancer investigation since several proteins known to be involved in human cancer development are thought to serve as substrates for FTase and to require farnesylation for proper biological activity. Several FTase inhibitors (FTIs) have advanced into clinical testing. Nevertheless, despite the progress in the field several functional and mechanistic doubts on the FTase catalytic activity have persisted. This work provides some crucial information on this important enzyme by describing the application of molecular dynamics simulations using specifically designed molecular mechanical parameters for a variety of 22 CaaX peptides known to work as natural substrates or inhibitors for this enzyme. The study involves a comparative analysis of several important molecular aspects, at the mechanistic level, of the behavior of substrates and inhibitors at the dynamic level, including the behavior of the enzyme and peptides, as well as their interaction, together with the effect of the solvent. Properties evaluated include the radial distribution function of the water molecules around the catalytically important zinc metal atom and cysteine sulfur of CaaX, the conformations of the substrate and inhibitor and the corresponding RMSF values, critical hydrogen bonds, and several catalytically relevant distances. These results are discussed in light of recent experimental and computational evidence that provides new insights into the activity of this enzyme.

Keywords Farnesylation · Force field · FTase · FTIs · Mechanism · Molecular dynamics · Zn enzymes

Introduction

Protein farnesyltransferase (FTase) has received much attention in the past few years for its importance in the context of cancer and more recently in parasitic and viral infections. FTase is a heterodimer consisting of a 48 kDa α-subunit and a 46 kDa β-subunit [1–5]. This enzyme contains a single zinc ion per protein dimer [6] that is essential for its catalytic activity [7]. FTase catalyses the post-translational addition of a hydrophobic isoprenoid farnesyl moiety from farnesyl diphosphate (FPP) to a cysteine residue of a protein substrate containing a typical -CaaX motif at the carboxyl terminus. In this conserved motif C represents the cysteine residue that is farnesylated, "a" is an aliphatic amino acid, and X represents the terminal amino acid residue, usually alanine, serine, methionine, or glutamine [8]. This process, called farnesylation, is a particular type of a more general form of lipid modification called protein prenylation that has been shown to be critical for the biological function of several proteins involved in signal transduction, as it is very important in membrane association and in protein-protein interactions [9]. Small variations in this CaaX motif transform the resulting peptides into substrates of different affinity, or into non-substrates/inhibitors for FTase.

Electronic supplementary material The online version of this article (doi:10.1007/s00894-012-1590-1) contains supplementary material, which is available to authorized users.

S. F. Sousa (✉) · J. T. S. Coimbra · D. Paramos · R. Pinto · R. S. Guimarães · V. Teixeira · P. A. Fernandes · M. J. Ramos
REQUIMTE, Departamento de Química e Bioquímica,
Faculdade de Ciências, Universidade do Porto,
Rua do Campo Alegre, s/n,
4169-007 Porto, Portugal
e-mail: sergio.sousa@fc.up.pt

M. J. Ramos
e-mail: mjramos@fc.up.pt

The discovery that the Ras proteins are modified by FTase and involved in the Akt signaling pathway that promotes cell proliferation, and mainly the fact that such modification is essential for the oncogenic forms of these proteins to be able to transform cells [10–12], has promoted widespread interest in protein farnesylation. Mutant Ras proteins (mutant H-, N- K-Ras) are responsible for about 30 % of all human cancers [13, 14]. They are particularly prevalent in pancreatic adenocarcinomas (implicated in ca. 90 % of all cases reported), colon adenocarcinomas and adenomas (ca. 50 %), lung adenocarcinomas (ca. 30 %), myeloid leukemias (ca. 30 %), and melanomas (ca. 20 %) [13–18]. In fact, mutations of the ras gene are early events in the development of cancer. The different Ras proteins differ between each other, among other features in the amino acid composition of their CaaX motif, and play a pivotal role in the transduction of cell growth-stimulating signals. Mutation of the ras gene leads to constant activation of the protein, ultimately resulting in uncontrolled cell proliferation [19]. Thus, blocking Ras proteins farnesylation quickly developed as a very promising strategic approach for the development of new anticancer drugs — the farnesyltransferase inhibitors (FTIs) [20–24]. By inhibiting Ras farnesylation, a blockade of the signal transduction pathway is accomplished with cessation of cell growth, ultimately resulting in cell growth arrest [21]. By doing so, FTIs are an emerging class of biologically active anticancer drugs. The exact mechanism of action of this class of agents is, however, currently unknown. In preclinical models, farnesyltransferase inhibitors showed great potency against tumor cells; yet in clinical studies, their activity was far less than anticipated [20, 21, 25, 26].

K-Ras, the most frequently mutated form of Ras in human cancers, which contains the CaaX motifs CVIM and CIIM, is able to bypass the FTI blockade through cross-prenylation by the related enzyme geranylgeranyltransferase I (GGTase I) [27–29]. Indeed, GGTase I targets a very large number of CaaX proteins that are important for cellular viability. The inhibition of this enzyme induces too many toxic effects to be used as a practical strategy, limiting the therapeutic benefit that might be gained by inhibiting oncogenic K-Ras through dual prenyltransferase inhibitor therapy [30].

A structural analysis of most important FTIs shows that all of them bind the FTase active site at the position occupied by the Caa portion of the CaaX peptide substrate motif, leaving free the X residue binding pocket (sometimes referred to as the “specificity pocket”) that accounts for the binding specificity of FTase in relation to GGTase I (as both enzymes differ on the preference for low affinity peptides with different amino acid residues at this position) [20]. In addition, the X-ray crystallographic structures for the FTase-FPP-FTI complexes reveal that the main inhibitors are only 60–70 % buried by FTase and FPP molecules, leaving enough room available for the addition of extra functional groups, as a strategy to modulate important aspects such as toxicity, bioavailability, or stability, without significantly affecting the specificity or the ability to bind of these compounds. These aspects should be explored in the development of more effective FTIs [20, 22, 31–33].

The work here described represents a new outlook for FTase inhibition in a detailed and integrated molecular dynamics analysis of a set of 22 CaaX tetrapeptides in an attempt to rationalize several aspects occurring at the active-site of the enzyme, in particular substrate binding (both FPP and the peptide). The knowledge gained from this analysis yields key clues for a more global understanding of the binding and inhibition mechanism played by these peptides.

Computational methods

The AMBER 10.0 molecular dynamics package was used in all the molecular dynamics (MD) simulations performed for the complexes formed between FTase, FPP, and the 22 CaaX peptides evaluated. The 22 systems were prepared from the crystallographic structures with the best resolution, namely 1D8D (enzyme-CVIM) [34], 1TN7 (enzyme-CVIF) [35], 1JCR (enzyme-CVFM) [36], and 1TN8 (enzyme-CVLS) [35] (Table 1). The structures of those CaaX-complexes that were not available from the PDB, were modeled from the X-ray structure of the FTase complex with the most similar tetrapeptide, as indicated in Table 1. In some cases, FPP had to be modeled at the position of a FPP analogue, according to the PDB file used.

Conventional protonation states for all amino acids at pH 7 were considered. FPP was modeled in the deprotonated form. All the hydrogen atoms were added and counter-ions (Na^+) were employed to neutralize the highly negative charges of the systems (ranging from −18 to −20). The Leap program was used for this purpose. Each of these systems was then placed in rectangular boxes containing a minimum distance of 12 Å of TIP3P water molecules between the enzyme and the box side. The size of these 22 systems was of ca. 100,000 atoms.

A set of parameters specifically designed to allow a reliable treatment of the Zn coordination sphere formed during catalysis and based on DFT (B3LYP) and molecular mechanical calculations [37–39], crystallographic data [36, 40, 41], extended X-ray absorption fine structure (EXAFS) results [42], and on several other more recent mechanistic studies [43–48] were applied to the systems in study (Table 1). These parameters are described in detail elsewhere [49] and have been already used with success in the study of FTase [33, 50–53]. All systems were subjected to a four-stages

Table 1 Summary of the experimental data and computational results obtained from the analysis of the MD simulations for all the 22 CaaX tetrapeptides evaluated

Type	CaaX tetrapeptide	Natural substrate	PDB code	IC_{50}[a] (μM)	Reference	CaaX RMSF (Å)	Average end-to-end distance (Å)	Number of hydrogen bonds with the FPP pyrophosphate group
High affinity	CVFM		1JCR	<0.10	[59]	0.99±0.40	10.20±0.47	34
	CVYM		1JCR	0.10	[59]	0.50±0.16	10.17±0.51	24
	CIIM	K-RasA	1D8D	0.15	[59, 60]	0.70±0.23	10.47±0.40	36
	CAIM	Lamin B	1D8D	0.15	[59, 60]	0.56±0.17	10.29±0.49	37
	CVVM	N-Ras	1JCR	0.15	[60]	0.79±0.32	11.20±1.00	39
	CVIM	K-RasB	1D8D	0.15	[59, 60]	0.45±0.13	10.36±0.47	36
	CVLM		1TN8	0.15	[60]	0.46±0.17	9.77±0.50	29
	CSIM	Lamin A	1D8D	0.20	[60]	0.52±0.18	10.01±0.57	17
Intermediate affinity	CIFM		1JCR	0.26	[59]	0.72±0.30	9.58±0.41	27
	CIIC		1TN8	0.35	[60]	0.86±0.32	10.07±0.50	19
	CIIS		1TN8	0.35	[60]	0.76±0.30	10.28±0.54	34
	CVCM		1JCR	0.38	[59]	0.57±0.18	10.00±0.49	29
	CVWM		1JCR	0.40	[59]	0.44±0.13	10.27±0.47	38
	CVIF		1TN7	0.55	[59]	0.46±0.17	9.75±0.38	29
	CFIM		1D8D	0.55	[59]	0.65±0.21	9.99±0.38	27
Low affinity	CVIS	Transducin	1TN8	1	[59, 60]	0.50±0.17	9.98±0.46	23
	CCIF		1TN7	2.8	[59]	0.81±0.29	9.57±0.44	24
	CVLS	H-Ras	1TN8	3	[59, 60]	0.56±0.18	9.95±0.41	29
	CVIA		1D8D	5	[60]	0.84±0.29	11.37±0.96	39
	CVIL	Rap2B	1D8D	11	[60]	0.58±0.22	9.98±0.47	18
	CLIL		1D8D	17	[60]	0.53±0.20	11.12±0.33	38
	CAIL		1D8D	100	[60]	0.60±0.20	10.88±0.48	23

[a] all values were determined under the same experimental conditions, as described in [59, 60]

refinement protocol using the SANDER module of AMBER 10.0, in which the constraints on the enzyme were gradually removed. In the first stage (10,000 steps), 50 $kcal mol^{-1} Å^{-2}$ harmonic forces were used to restrain the positions of all atoms in the systems except those from the water molecules. In the second stage (10,000 steps), these constraints were applied only to the heavy atoms, and in the third stage (30,000 steps) were limited to the C_α and N atom-type atoms (backbone α-carbon and nitrogen atoms). This process ended in a full energy minimization (4th stage, maximum 80,000 steps) until the rms gradient was smaller than 0.02 $kcal mol^{-1}$.

MD simulations were carried out using the PMEMD module of AMBER 10.0, and considering periodic boundary conditions to simulate a continuous system. The SHAKE algorithm was applied to fix all bond lengths involving a hydrogen atom, permitting a 2-fs time step. The Particle-Mesh Ewald (PME) method was used to include the long-range interactions, and a non-bond interaction cut-off radius of 10 Å was considered. Following a 100 ps equilibration procedure, 10 ns MD simulations were carried out at 300 K using the Berendsen temperature coupling scheme at constant pressure (1 atm) with isotropic molecule-based scaling, resulting in a total simulation time of 220 ns. The MD trajectory was sampled every 2.0 ps. All of the MD simulations were analysed with the PTRAJ module of AMBER 10.0, with values retrieved from the last 8 ns of the simulation.

Results and discussion

Experimental IC_{50} values

IC_{50} represents the half maximal inhibitory concentration and corresponds to the quantity of a particular drug or inhibitor that is required to inhibit a given biological process by half. It is therefore a measure of the effectiveness of a compound in inhibiting a biological or biochemical function such as the activity of an enzyme, with lower IC_{50} values indicating more effective compounds. Taking into account the experimental IC_{50} values described in the literature and the MD simulations performed (Table 1), we searched for potential features that could point out possible inhibition mechanisms and to influence the binding ability of the different tetrapeptides. For this purpose, we have decided

to group CaaX tetrapeptides as potential high affinity peptides (IC_{50} values ranging between 0.10 and 0.20 μM), intermediate affinity peptides (IC_{50} values ranging 0.26–0.55 μM) and low affinity peptides (IC_{50} values above 1.0 μM).

RMSd analysis

Figure 1 illustrates the C_α root mean square deviation (RMSd) variation with time in all the MD simulations performed. The results show that all the systems are well equilibrated after the initial 2 ns in both simulations. In agreement with this observation the last 8 ns on all simulations were taken into consideration for the calculation of the values in the subsequent sections.

RMSF analysis

A root mean square fluctuation (RMSF) analysis allows an identification of the more flexible regions and also a comparison of the relative flexibility of different parts of a system. In this study, we have analyzed the flexibility changes during the MD simulations in an attempt to reveal some important trends for each of the tetrapeptides. RMSF analysis shows an immediate feature concerning the sequence similarity of CaaX tetrapeptides and the variation pattern of RMSF values (Figs. 2 and 3). For each group of tetrapeptides, the RMSF at the C_α of each residue was taken into consideration for the determination of the average flexibility for each helix (FTase has a total of 29 helices — 15 in the α-subunit and 14 in the β-subunit — as illustrated in Fig. 2). The flexibility of the C_α amino acid residue along the CaaX sequence for each tetrapeptide was compared for each one of these classes of tetrapeptides (Fig. 3). These representations were further complemented with a tridimensional view on the average flexibility patterns associated to each of these three groupings (Fig. 4).

Analysis of the general flexibility pattern of FTase α and β subunit helices (Fig. 2) and of the tetrapeptides (Fig. 3) and the corresponding tridimensional view (Fig. 4) allows a

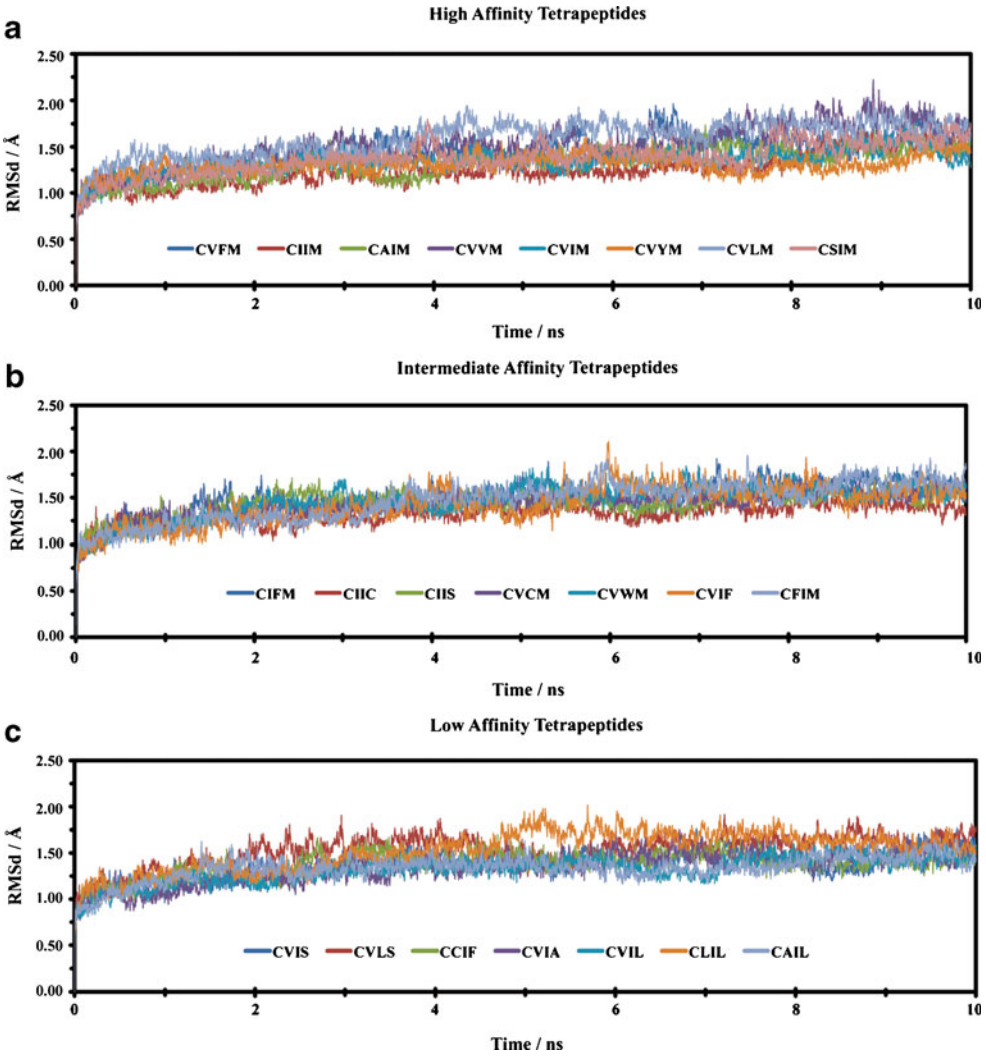

Fig. 1 RMSd representation of the protein C_α atoms as a function of time for the 22 FTase MD simulations with the CaaX peptides grouped into: **a** high affinity tetrapeptides; **b** intermediate affinity tetrapeptides; **c** low affinity tetrapeptides

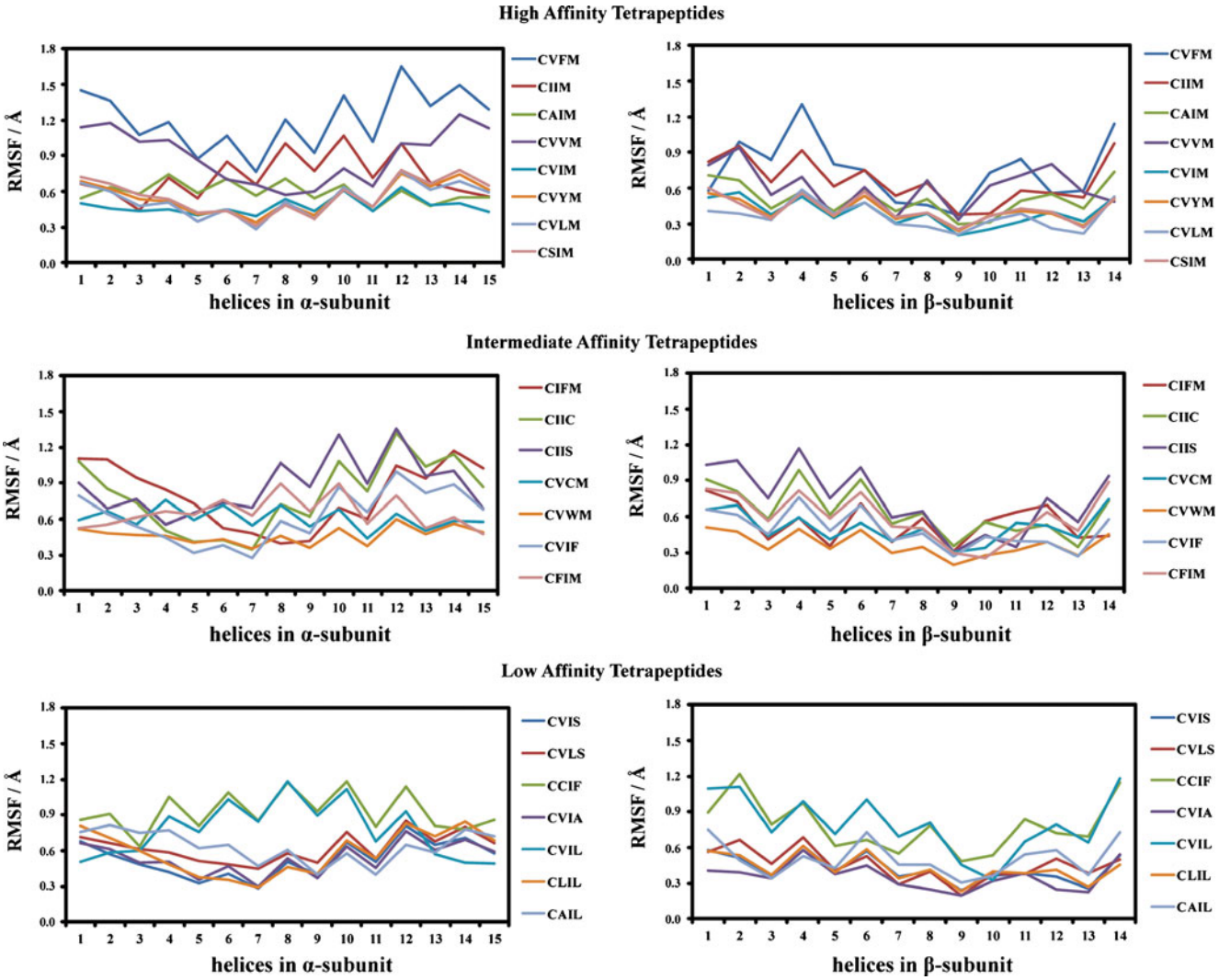

Fig. 2 RMSF analysis for all the amino acid residues along the FTase sequence calculated for the last 8 ns of the MD simulations performed for each of the 22 FTase-tetrapeptide complexes. The values for each helix refer to the average values calculated for all the amino acid residues present in each helix

definition of some common patterns concerning the localization of the most flexible regions in both subunits and of the tetrapeptide itself. In general, these representations show that the active-site region, including the Zn coordination sphere and the amino acid residues that account for most of the interactions with the peptides, have a low average flexibility compared with the remaining of the enzyme. In contrast, some regions with higher flexibility are observed at the surface of the enzyme, mainly in the β-subunit (Fig. 4).

In respect to the CaaX putative FTase low affinity peptides, with high IC_{50} values (CVIA, CVIL, CCIF, CLIL, CAIL, CVIS and CVLS), they present, in general, higher RMSF values (Tables 1 and 2). Five of the seven low affinity peptides considered have average RMSF values between 0.56 and 0.84 Angstroms. The exceptions are CVIS (0.50) and CLIL (0.53). In CVIA, CCIF, CLIL, CVIS and CVLS, the most flexible helices emerge on the enzyme's surface, not resembling any critical role in the flexibility of the active site. Only in CVIL the 14β helix is found in the vicinity of the active site and the last two residues (isoleucine and leucine) show low RMSF values when compared to the first two residues. The same pattern is observed in CCIF relatively to the flexibility of the tetrapeptide. A more detailed analysis demonstrates that for both α and β subunits, there is a reasonable consistency in the pattern of CaaX tetrapeptides in terms of RMSF variation, as it can be observed, for instance, for 1α, 2α, 3α, 4α and 5α helices. Such pattern can reveal itself important for this parameter for the distinction between low and intermediate to high affinity peptides. Table 3 presents the average RMSF values for each helix in each of the groups of peptides analyzed.

Concerning the putative high affinity peptides (CVIM, CIIM, CAIM, CSIM, CVFM, CVYM, CVVM and CVLM), all of them differ in the second or third residue. These

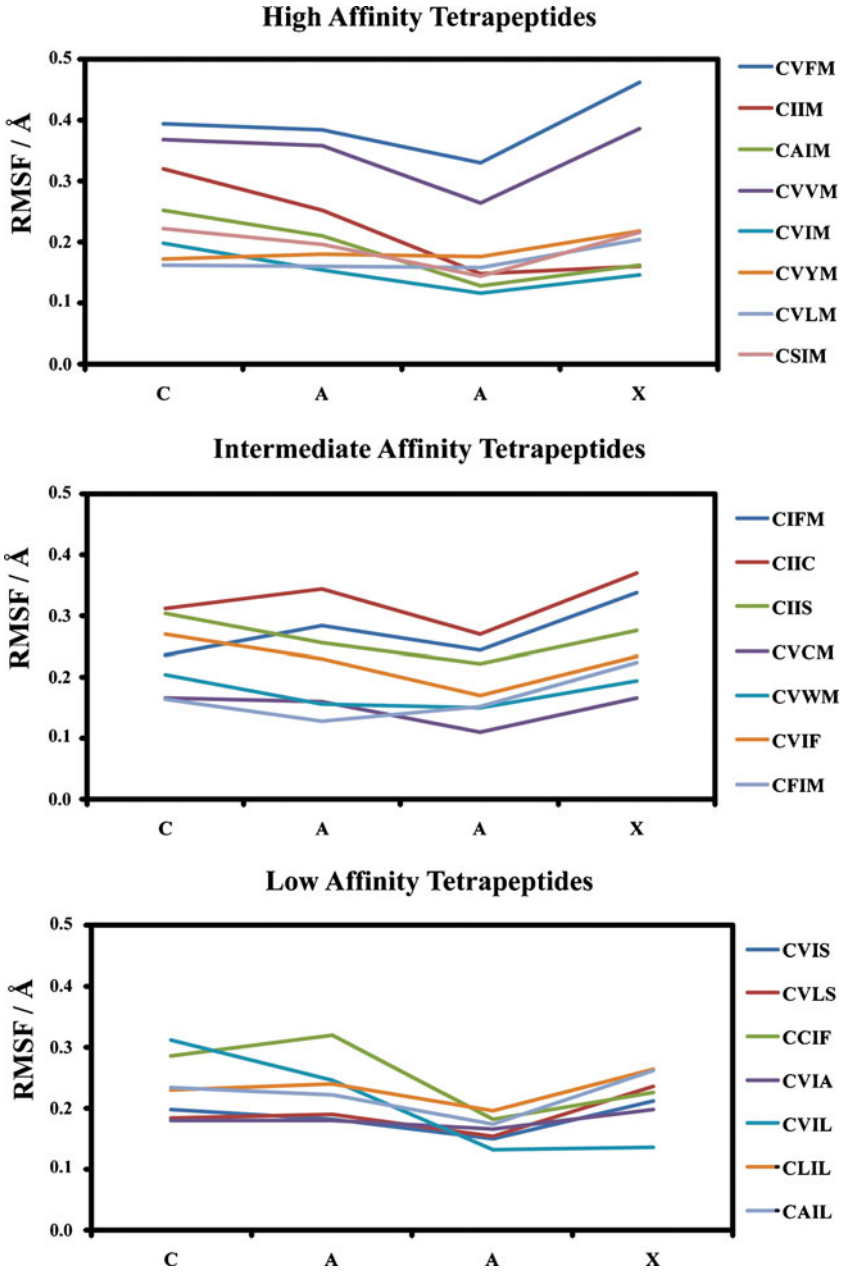

Fig. 3 RMSF analysis for all the four amino acid residues along the CaaX sequence for each of the 22 FTase-tetrapeptide complexes evaluated, calculated from the last 8 ns of the MD simulations performed

tetrapetides tend to present lower RMSF values, on average (Table 2), than the other two groups of tetrapetides. Five of the eight high affinity peptides analyzed have average RMSF values between 0.45 and 0.56 Angstrom. The exceptions are CIIM (0.70), CVVM (0.79) and most of all CVFM (0.99). Analyzing the individual helices in detail, it can be observed that in CAIM the most flexible helices are 4α and 14β (Fig. 2), close to the active site and the same occurs with 14β helix of the enzyme with which CIIM is interacting. Moreover, these two peptides show a similar variation pattern in RMSF values along the tetrapeptides chain with the lowest values in the two last residues (see Fig. 3). The other mentioned tetrapeptides do not seem to induce a high flexibility in the enzyme, particularly in the active site, since the most flexible helices are exposed to the surface, in contact with solvent, a pattern already observed for the last peptides mentioned. Interestingly, CAIL, previously defined as a low affinity peptide according to its IC_{50} value, shows similar behavior — the most flexible helices are in relative proximity to the active site. From this group, only CVFM and CVVM show high RMSF values for the tetrapeptide and CVFM in particular, shows the highest RMSF values of all, both for the helices of the enzyme and for the tetrapeptide itself, an aspect that can be of crucial importance since peptide coordination induces an increase in the flexibility of the pyrophosphate moiety, although decreasing the

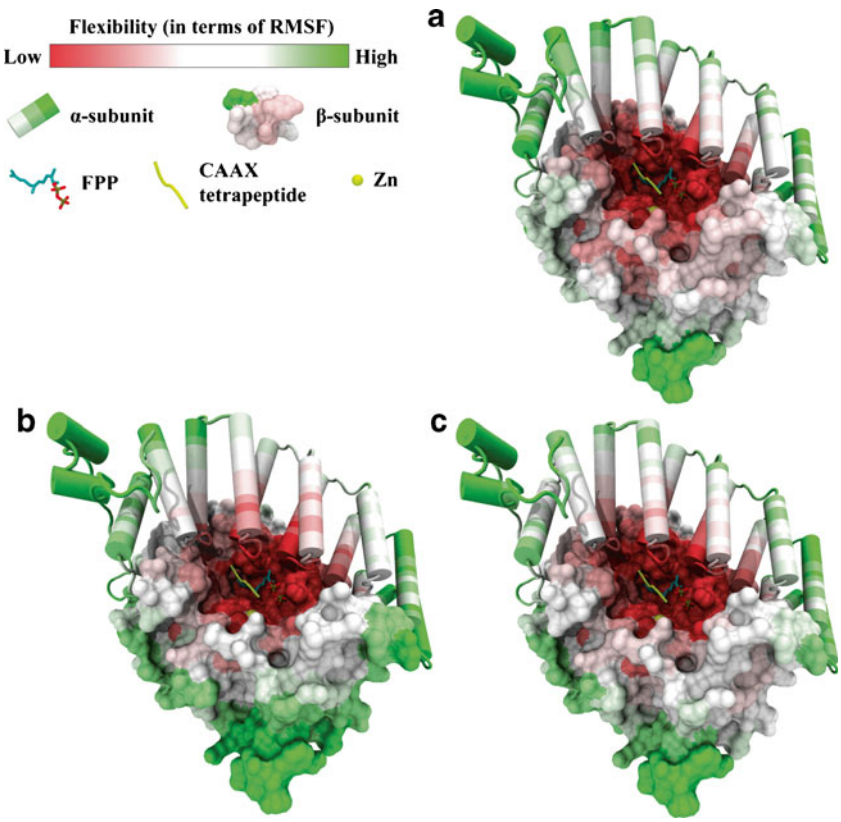

Fig. 4 Tridimensional representation of the average RMSF values for each class of peptides, as calculated from the last 8 ns of each of the 22 MD simulations performed. **a** high affinity peptides; **b** intermediate affinity peptides; **c** low affinity peptides

flexibility of the farnesyl portion of FPP. Interestingly, this peptide has been shown to be the most potent CaaX tetrapeptide inhibitor [20].

Finally, for the presumed intermediate affinity peptides (CIIC, CIIS, CVIF, CFIM, CVWM, CVCM and CIFM), the analysis is reasonably eased, although the range of average flexibility for each tetrapeptide is quite significant (Table 1). In all of them, at least one of the most flexible helices is relatively close to the active site. In addition, for CIIC, CIIS, CFIM and CIFM, they present intermediate-to-high RMSF values for these four tetrapeptides, which, concomitantly with the results for the helices, opposes the behavior presented by putative low affinity peptides.

Considering the high RMSF values observed for low affinity peptides, we can establish that such feature is in agreement with the previous observation that peptide coordination causes a decrease in the flexibility of the whole enzyme, which would be followed by an increase in flexibility that takes place upon product formation, if any, although the main structural and dynamical properties of the active site are not significantly altered [50, 52]. These events lead to major changes in flexibility at the most external regions of the enzyme because a relatively small change at the active site is amplified into a much more significant alteration at the external surface of the enzyme, and this can possibly be an explanation of what is observed in surface helices [52]. Moreover, it is known that peptide coordination induces a decrease in the flexibility of the farnesyl portion of FPP [50, 52]. On the other hand, at least for some intermediate affinity peptides, we can observe that the most important alterations occur in the vicinity of the active-site. FPP binding to FTase has also been anticipated to be important for the binding of several promising FTIs, as recently demonstrated in solution for Lonafarnib [54]. Moreover, it is clear for the majority of the cases that the most flexible helices are 12α and 4β (Fig. 2). Interestingly, these helices have a lower percentage of highly-conserved residues (0–15 %), as previously described [52]. In fact, the magnitude of the changes induced by the alterations taking place at the active-site are particularly large for a set of poorly conserved helices located considerably away from the active site, in particular for helices 12α and 4β. As is observed, the induction of the enzyme's flexibility by potential FTase inhibitors or natural substrates with these

Table 2 Summary of the average results obtained from the analysis of the MD simulations for the different groups of CaaX tetrapeptides evaluated

Type	Average CaaX RMSF (Å)	Average end-to-end distance (Å)	Average number of hydrogen bonds with the FPP pyrophosphate
High affinity	0.62	10.3	31.5
Intermediate affinity	0.64	10.0	29.0
Low affinity	0.63	10.4	27.7

Table 3 Summary of the average RMSF results (in Angstrom) and standard deviation errors for the different α and β subunit helices depending on the affinity of the tetrapeptides. Some peptides were excluded due to the disparity of the profiles: CVFM and CVVM for the high affinity peptides; and CCIF and CVIL for the low affinity peptides

Helices	α subunit			β subunit		
	High affinity	Intermediate affinity	Low affinity	High affinity	Intermediate affinity	Low affinity
1	6.30±0.89	7.90±2.51	7.24±0.60	6.02±1.47	7.73±1.75	5.72±1.22
2	5.96±0.73	7.11±2.03	6.75±0.94	5.90±2.02	7.39±1.84	5.17±0.98
3	5.06±0.65	6.60±1.64	5.88±1.08	4.13±1.21	5.04±1.38	3.77±0.50
4	5.77±1.22	6.06±1.53	5.54±1.37	6.18±1.47	7.74±2.39	6.05±0.56
5	4.49±0.93	5.37±1.54	4.41±1.25	4.14±1.00	5.04±1.54	4.00±0.18
6	5.56±1.80	5.69±1.62	4.73±1.13	5.66±1.01	7.38±1.84	5.74±1.03
7	4.25±1.51	4.76±1.56	3.58±0.93	3.74±0.88	4.52±1.05	3.46±0.67
8	6.25±2.04	6.93±2.35	5.37±0.56	4.31±1.26	5.26±1.03	3.82±0.79
9	4.83±1.56	5.66±1.69	4.15±0.50	2.64±0.65	2.91±0.50	2.35±0.44
10	7.01±1.81	8.64±2.64	6.66±0.65	3.36±0.48	4.10±1.25	3.64±0.28
11	5.00±1.08	6.23±1.90	4.86±0.60	4.34±0.91	4.54±1.14	4.13±0.72
12	7.59±1.39	9.67±3.04	7.83±0.78	4.25±1.11	5.60±1.40	4.19±1.29
13	5.92±0.88	7.53±2.41	6.50±0.55	3.39±1.13	3.99±1.08	3.01±0.71
14	6.45±1.10	8.52±2.66	7.64±0.65	6.30±1.90	6.82±1.99	5.52±1.03
15	5.66±0.79	6.87±2.00	6.48±0.61			

particular regions should be taken into account for the development of more specific inhibitors. Also by the analysis of Fig. 3, the third residue of the tetrapeptide is the one which exhibits the lower RMSF value in most cases, while the higher can be any of the others, depending on the particular peptide composition. This viewpoint suggests a presumed important role and is biologically significant of the third residue in the peptide stabilization at the active site and possibly in the design of more potent FTIs.

A more comprehensive scrutiny of Fig. 2 shows a very consistent pattern for both α and β subunits and simultaneously the most reliable panorama of all groups of peptides. Once again, this pattern proves to be quite consistent for the distinction between intermediate and high affinity peptides, in particular. A more heterogeneous patter for CaaX amino acids can be observed from the analysis of Fig. 3.

Because of the difficulty in the investigation of similar patterns between the tetrapeptides known to have similar IC_{50} values, the relation between a given flexibility pattern and the behavior of the tetrapeptide as an inhibitor or a simple substrate of FTase remains uncertain, though some features could be established. Thus, together with the RMSF analysis, more aspects of the interaction need to be clarified in order to establish a relationship with the inhibitory profile.

Analysis of some important hydrogen bonds between water molecules and FPP

Another important feature concerning peptide association are the hydrogen bonds established between the pyrophosphate moiety of FPP and water molecules and surrounding amino acid residues, as FPP is known to form an important part of the binding pocket for the CaaX substrates. Table 1 indicates the most relevant hydrogen bonds formed with the pyrophosphate moiety of FPP and some water molecules and amino acid residues that seem to be important for the association mechanism. Only the hydrogen bonds that were present during more than 5 % of the total simulation time are included.

From the analysis of Table 1, an immediate difference arises concerning the total number of hydrogen bonds stabilizing the oxygen atoms of the pyrophosphate moiety of FPP for each tetrapeptide, as can be observed, for instance, for CVVM (39 hydrogen bonds) and CSIM (17 hydrogen bonds). In order to optimize the analysis and obtain a more comprehensive view, we have established a distribution pattern by which the peptides are organized according to intervals of the number of hydrogen bonds (Table 1). From this distribution, we ascertain a group of peptides, namely CVIL, CSIM, CAIL, CVIS, CVYM, CCIF and CIIC that establish 17 to 24 hydrogen bonds, another group, specifically CVLM, CVLS, CVCM, CIFM, CVIF and CFIM with 27 to 29 hydrogen bonds and finally the most ample group that comprises some peptides such as CLIL, CVFM, CVWM, CVVM, CVIA, CIIS, CVIM, CIIM, CAIM, that exhibit 34 and 39 hydrogen bonds. According to experimental data (IC_{50} values), an immediate correlation can be made.

Indeed, the analysis of the first group demonstrates that most peptides present are low affinity peptides. On the other hand, the second group above is constituted by

intermediate- to-high affinity peptides, although most of them are considered to be of intermediate affinity and in particular CVLM is pointed to be a higher affinity peptide than the remaining ones. The third group is mostly comprised of high affinity peptides (lowest IC_{50} values), with only some exceptions. This analysis allows one to discriminate between peptides that may function as low affinity peptides, corresponding to the first group, those peptides with an intermediate activity, that includes the second group, and finally the third group which embrace CaaX tetrapeptides with a higher affinity, although some exceptions can be observed. In addition, the procedure also allowed the peptides that establish a significant number of hydrogen bonds to be grouped according to the specific pattern above described. Most of the high affinity peptides exhibit hydrogen bonds with percentages of occupancy above 50.0 % such as CVCM, CVIF, CVFM, CIIC, CFIM, CVWM, CVVM and CVIM (Table 1). Therefore in these peptides, the pyrophosphate group from the FPP is highly stabilized, with the FPP pyrophosphate moiety in a position that favors the formation of hydrogen bonds with water molecules and amino acid residues at the binding pocket.

Previous modeling studies have shown that the pyrophosphate moiety of FPP undergoes a major increase in the flexibility induced by peptide coordination, although the flexibility of the farnesyl portion of FPP decreases. This higher positional variation seems to be important for the chemical step catalyzed by the enzyme involving pyrophosphate exit and a conformational rearrangement of the first two isoprenoid subunits of FPP, a change that is maximal for the pyrophosphate bound carbon 1 of the farnesyl portion of FPP, which is ultimately connected to the Zn-bound sulfur atom of the peptide's cysteine to originate the farnesylated peptide product [5, 50]. On the other hand, computational evidence has proved that in the binary complex, most of the hydrogen bonds of the pyrophosphate moiety are established with rapidly exchanging water molecules and therefore the number of persistent hydrogen bonds is very small [50]. The analysis of Table 1 on this point has demonstrated a good correlation between the binding affinity of some peptides and the number of hydrogen bonds between the pyrophosphate moiety of FPP and water molecules around. The average values presented in Table 2 further confirm these conclusions.

These observations suggest a possible mechanism by which the CaaX inhibitors tend to establish a greater number of hydrogen bonds that would be less transient and would stabilize the pyrophosphate moiety in such a way that the ternary complex (FTase-FPP-CaaX) would become more stable and the farnesylation reaction that occurs during the catalytic mechanism, would be less likely to happen and would occur more slowly. Therefore, the quantity of farnesylated product formed would be lower. Additionally, we can speculate that a higher number of hydrogen bonds would also decrease the flexibility of pyrophosphate moiety, since we assume that these would be less transient and that therefore would present a higher average lifetime, meaning that the increase of flexibility of the pyrophosphate moiety would be less pronounced.

Analysis of some important hydrogen bonds between enzyme residues and FPP

Table 4 describes the most relevant hydrogen bonds formed between active-site amino acid residues and FPP and pyrophosphate moiety of FPP. Only the hydrogen bonds that were present during more than 30 % of the total simulation time are included in this particular table. For a more comprehensive panorama, we have also determined the nature of interactions between FPP and water by including the analysis of the hydrogen bonds that were present during more than 30 % of the total simulation time between oxygen atoms of pyrophosphate moiety of FPP and water molecules.

From the analysis of Table 4, an immediate feature can be established concerning the nature of the amino acid residues that are present at the active site. Some of these residues form a positively charged pocket that is defined by the amino acid residues Lys164α, His248β, Arg291β, Lys294β and His201α, which are significantly less exposed to the solvent. These amino acid residues, mainly Lys164α, Arg291β, and Lys294β, have already been pointed out to play some role in FPP binding at the binary complex and are more sensitive to pyrophosphate removal, which occurs with the formation of the product complex [50].

Previous computational work has shown low RMSF values for this residue in the FTase product state, demonstrating that the flexibility of this residue is sensitive not only to the pyrophosphate position, but also to the conformation of the remaining portion of FPP. These results also highlighted Lys164α as the most important pyrophosphate stabilizing residue in the FTase catalytic cycle [50], as it is the residue that establishes the highest number of hydrogen bonds, although usually with low percentages of occupancy (10–20 %), and that reacts more strongly to the alterations taking place at the active-site.

In order to analyze the behavior and establish a distribution pattern of all peptides, we have analyzed the MD simulations and the effect of solvent on FPP binding promoted by peptide coordination. In addition, we have focused on the nature of hydrogen bonds that are established between each amino acid residue and FPP and water molecules with the oxygen atoms of the pyrophosphate moiety of FPP in order to find a potential pattern.

For the group identified as low affinity peptides, we observed a persistent hydrogen bond established between Arg291β and the O1A and O2B pyrophosphate oxygen

Table 4 Summary of the most relevant hydrogen bonds formed between the FPP molecule and the active-site amino acid residues and water molecules. Only the amino acid residues with an occupation score above 30 % and water molecules with an occupation score superior to 50 % are depicted. AMBER standard nomenclature used in atomic description

HIGH AFFINITY TETRAPEPTIDES

CVFM

acceptor	donor atoms			%
atoms	residue	atom1	atom2	occupation
O2B	Arg291β	HH21	NH2	78.12
O1B	Arg291β	HH21	NH2	53.65
O1A	H_2O	H2	O	56.85
O2B	H_2O	H1	O	50.10

CIIM

acceptor	donor atoms			%
atoms	residue	atom1	atom2	occupation
O1B	Arg291β	HH21	NH2	79.28
O2B	Arg291β	HE	NE	76.73
O2B	Arg291β	HH21	NH2	75.20
O2B	His248β	HE2	NE2	62.30
O2A	Tyr300β	HH	OH	49.97

CAIM

acceptor	donor atoms			%
atoms	residue	atom1	atom2	occupation
O1B	Arg291β	HH21	NH2	50.38

CVVM

acceptor	donor atoms			%
atoms	residue	atom1	atom2	occupation
O2B	Arg291β	HH21	NH2	85.10
O2B	H_2O	H2	O	59.20
O2B	Arg291β	HE	NE	53.85
O3B	Tyr300β	HH	OH	47.28
O1B	Arg291β	HH21	NH2	45.00

CVIM

acceptor	donor atoms			%
atoms	residue	atom1	atom2	occupation
O3B	Arg291β	HH21	NH2	76.23

CVYM

acceptor	donor atoms			%
atoms	residue	atom1	atom2	occupation
O2A	Arg291β	HH21	NH2	80.20
O1A	Arg291β	HE	NE	53.78
O1A	**Arg291β**	**HH21**	**NH2**	**40.60**

CVLM

acceptor	donor atoms			%
atoms	residue	atom1	atom2	occupation
O2B	Arg291β	HH21	NH2	61.08
O1B	**Arg291β**	**HH21**	**NH2**	**43.25**

INTERMEDIATE AFFINITY TETRAPEPTIDES

CIFM

acceptor	donor atoms			%
atoms	residue	atom1	atom2	occupation
O1B	Arg291β	HH21	NH2	46.20

CIIC

acceptor	donor atoms			%
atoms	residue	atom1	atom2	occupation
O1A	Arg291β	HH21	NH2	82.40
O1	His248β	HE2	NE2	76.48
O2A	H_2O	H1	O	57.38
O1A	H_2O	H1	O	53.22
O1A	Arg291β	HE	NE	51.50

CIIS

acceptor	donor atoms			%
atoms	residue	atom1	atom2	occupation
O2B	Arg291β	HH21	NH2	74.15

CVCM

acceptor	donor atoms			%
atoms	residue	atom1	atom2	occupation
O1B	H_2O	H1	O	82.82
O2B	Arg291β	HH21	NH2	78.90
O1B	Arg291β	HH21	NH2	76.13
O2B	Arg291β	HE	NE	73.00
O1A	H_2O	H2	O	70.23
O3A	His248β	HE2	NE2	55.35

CVWM

acceptor	donor atoms			%
atoms	residue	atom1	atom2	occupation
O1A	Arg291β	HH21	NH2	80.15
O1A	H_2O	H1	O	77.57
O2A	Arg291β	HH21	NH2	54.72
O1	His248β	HE2	NE2	51.15

CVIF

acceptor	donor atoms			%
atoms	residue	atom1	atom2	occupation
O2A	H_2O	H1	O	70.13
O1A	H_2O	H2	O	69.70
O1A	Arg291β	HH21	NH2	68.48
O1	His248β	HE2	NE2	64.72
O1A	Arg291β	HE	NE	45.20

CFIM

acceptor	donor atoms			%
atoms	residue	atom1	atom2	occupation
O1A	Arg291β	HH21	NH2	83.55
O1	His248β	HE2	NE2	72.80
O1A	H_2O	H2	O	63.98
O1A	Arg291β	HE	NE	53.80

CSIM

acceptor	donor atoms			%
atoms	residue	atom1	atom2	occupation
O1	His248β	HE2	NE2	75.38
O2A	Arg291β	HH21	NH2	65.05
O1A	Arg291β	HH21	NH2	62.20
O1A	Arg291β	HE	NE	60.68
O2A	H_2O	H1	O	54.93

LOW AFFINITY TETRAPEPTIDES

CVIS

acceptor	donor atoms			%
atoms	residue	atom1	atom2	occupation
O2A	Tyr300β	HH	OH	75.17
O1B	H_2O	H1	O	70.53
O2B	Arg291β	HH21	NH2	61.22

CVLS

acceptor	donor atoms			%
atoms	residue	atom1	atom2	occupation
O2B	**Arg291β**	**HH21**	**NH2**	**36.65**
O2A	Tyr300β	**HH**	**OH**	**33.30**
O2A	**Arg291β**	**HH21**	**NH2**	**33.02**

CVIA

acceptor	donor atoms			%
atoms	residue	atom1	atom2	occupation
O2B	Arg291β	HH21	NH2	94.85
O2B	H_2O	H2	O	69.67

CCIF

acceptor	donor atoms			%
atoms	residue	atom1	atom2	occupation
O2B	Arg291β	HH21	NH2	77.05
O2B	Arg291β	HE	NE	76.38
O3B	H_2O	H1	O	76.38
O1A	H_2O	H1	O	73.83
O3B	Tyr300β	HH	OH	63.88
O1B	Arg291β	HH21	NH2	58.95

CVIL

acceptor	donor atoms			%
atoms	residue	atom1	atom2	occupation
O1A	Arg291β	HH21	NH2	78.57
O2A	H_2O	H1	O	64.40
O1A	H_2O	H2	O	56.17
O1	His248β	HE2	NE2	50.35
O2A	**Arg291β**	**HH21**	**NH2**	**43.20**

CLIL

acceptor	donor atoms			%
atoms	residue	atom1	atom2	occupation
O2B	Arg291β	HH21	NH2	83.03
O1B	**Arg291β**	**HH21**	**NH2**	**44.70**
O2B	**Arg291β**	**HE**	**NE**	**43.40**

CAIL

acceptor	donor atoms			%
atoms	residue	atom1	atom2	occupation
O1A	H_2O	H1	O	60.22
O2A	H_2O	H2	O	56.70
O1	His248β	HE2	NE2	51.32
O1A	Arg291β	HH21	NH2	48.15

atoms, although the last bond is the most prevalent and consistent of these interactions. These hydrogen bonds are present during percentages of occupancy values that are around 70.0 %. However, some residues, such as His248β and Tyr300β, do not seem to be imperative since there are almost no important interactions with both amino acids, although some exceptions can be observed. The CAIL and CVIL peptides appear to establish an important interaction

between the histidine residue and the pyrophosphate moiety of FPP with a percentage of occupancy of approximately 50.0 %. CVIS and CCIF exhibit a central hydrogen bond between O2A and the pyrophosphate oxygen of FPP and Tyr300β with a 75.2 % and 63.9 % of occupancy, respectively, which represents some of the highest values of percentage presented for both peptides. Thus, it can be established that these interactions may be essential for the particular behavior of these low affinity peptides. In addition to these active-site amino acid residues, there are also some persistent water molecules that establish hydrogen bonds mainly with the O2A and O2B pyrophosphate oxygen of FPP.

For the set of CaaX peptides that behave like intermediate affinity peptides, we observe a persistent hydrogen bond established between Arg291β and the O1A and O2B pyrophosphate oxygen atoms, though the previous bond is the most prevalent and consistent of these interactions, contrary to that previously observed in the group of low affinity peptides. These hydrogen bonds are present during percentages of occupancy values that are around 67.0 %, although there is a more variable set of values than the other group mentioned above. Residues His248β and Tyr300β appear to be crucial since there are persistent interactions with both amino acids. Indeed, there are relevant interactions between O1 and O3A pyrophosphate oxygen atoms and His248β with percentages of occupancy ranging from 55.4 % (CVCM) and 76.5 % (CIIC). Such perspective is not observed for the previous peptides. As it was observed for low affinity peptides, Tyr300β does not seem to be important, contrarily to His248β. In CIIC, it is possible to observe that an important interaction is established with the histidine residue with a percentage of occupancy of 76.5 %. However, some exceptions exist. The CIFM and CIIS do not establish any important interaction between the histidine residue and pyrophosphate moiety of FPP; the same is observed for Tyr300β. Moreover, there are also some important water molecules that establish hydrogen bonds mainly with the O1A and O2A pyrophosphate oxygen of FPP.

Finally, the last set of peptides that are regarded as high affinity peptides, namely CLIL, CVFM, CVWM, CVVM, CVIA, CIIS, CVIM, CIIM, CAIM according to Table 1, a more heterogeneous scenario is observed, even though a pattern can be recognized. For Arg291β, we observed that the most prevalent interactions are established between O1B and O2B pyrophosphate oxygen atoms of FPP and the residue, although some interactions with O2A oxygen atom are observed. In opposition to the behavior of all peptides mentioned, these peptides present the highest values of percentage of occupancy with an average value above 80.0 % when considered the interaction with the highest percentage. As observed for the low affinity peptides already mentioned, we observe the same pattern in a way that His248β does not seem to be important in most peptides. Some exceptions to this sample are shown in CVIM and CSIM structures, in which we observed some important interactions between O1 pyrophosphate oxygen atom and the residue with a percentage of occupancy of 62.3 % and 75.4 %, respectively. An additional hydrogen bond is also seen in CIIM peptide between O2B of FPP and the residue with a percentage of 55.4 %. Concerning Tyr300β, we can determine that no relevant interactions are established, although CIIM presents itself as an exception with a 50.0 % percentage of occupancy in respect to the interaction between O2A pyrophosphate oxygen and the amino acid residue. Furthermore, there are also some important water molecules that establish hydrogen bonds mainly with the O2B and O1A, although O2A pyrophosphate oxygen atom is also relevant in some cases. Some peptides, such as CAIM and CVIM, do not present important hydrogen bonds interactions at all.

Analysis of important distances

Table 1 shows the average distance between the nitrogen atom of cysteine residue (C) and the oxygen atom of carboxyl group of X aminoacid of the CaaX tetrapeptide (end-to-end distance). Here, a more general insight on the conformation patterns of tetrapeptides is sought, allowing one to evaluate for example which CaaX tetrapeptide tends to get a more compact or extended conformation at the FTase active-site.

Analysis of Table 1 shows that some peptides that exhibit some of the highest distance values (near 11.0 Å), and hence a more extended conformation, are considered to be low affinity peptides such as CAIL, CLIL and CVIA and show some important conformational changes on the FTase active site. On the other hand, some peptides that are also regarded as low affinity peptides (CVIS, CCIF and CVIL) exhibit the lowest values, which contrasts with the behavior previously established. One important feature arises from the RMSF analysis, which shows that these peptides present the same variation pattern of RMSF (Fig. 4), with the exception of CVIL, which exhibits a more complex behavior, so a pattern of conformation and flexibility can be reasonably established.

An important number of the CaaX peptides evaluated present an end-to-end distance pattern ranging between 10.0 and 11.0 Å and comprise a non-homogeneous group of peptides, although all of them belong to the group of intermediate-to high affinity, such as CVFM, CVWM, CVYM, CVIM, CAIM, CSIM and CIIM. Some peptides, like CVWM and CVYM, exhibit a lower average end-to-end distance and therefore a more compact conformation. Thus, a direct correlation cannot be made for all the peptides analyzed from this quantity only and the RMSF analysis proves to be more consistent and more important, particularly

in terms of the flexibility induced in the active-site after peptide coordination.

Nevertheless, we can speculate that a more extended conformation seems to be important for the significant alteration in the flexibility of the pyrophosphate moiety of FPP induced by peptide coordination. As an overall result, some peptides that behave as low affinity peptides have the highest distance values (Tables 1 and 2), adopting an extended conformation and showing an intermediate degree of flexibility, which suggests that for this particular set of peptides, this feature can be significant. By contrast, the other group that exhibits more compact conformations, such as CVFM, CVWM, and CSIM show a lower variation of distance and thus it may be important for a possible inhibition mechanism by inducing inconsequential changes of conformation at the active-site after peptide coordination. However, this parameter does not allow ascertaining a clear and direct comparison, even though it can prove to be an interesting aspect to be studied in the future for the development of FTase inhibitors.

Radial distribution function (RDF) analysis of water around catalytic zinc and cysteine sulfur (S) atom of CaaX tetrapeptide

The exact nature of the Zn coordination sphere in FTase has been elucidated by computational studies some years ago and it has proved to be central for the catalytic mechanism of this enzyme [37, 55, 56]. Some aspects of dealing with the arrangement of the zinc active site and some important features played by key residues in the active-site have become progressively clearer. Here, we intend to elucidate its importance on the inhibition mechanism by CaaX peptides.

As previously discussed in the literature, two Zn coordination hypotheses have been demonstrated to lie in notably close energetic proximity [5, 37]. The small energy differences together with a very small energetic barrier of the conversion between the two possible conformers suggested that a mono-bidentate change with water elimination is reversible and extremely fast, indicating that both coordination alternatives exist in equilibrium [57, 58]. This could imply that the Asp297β carboxylate group performs an important biological role by assisting ligand entrance and/or displacement to/from the zinc coordination sphere through a carboxylate-shift. A previous study has shown a RDF maximum at a suitable distance from the metal atom that makes it possible for equilibrium to occur, both in the case of the resting state of FTase and of the binary complex, with the Zn–OH_2 radius characterized on the average of 2.8 Å with a sharp peak [50]. On the other hand, such aspect was not observed for the ternary and product complexes, in which the radius was about 4.2 and 4.3 Å and the existing peaks were found to be much less pronounced [50].

Taking this into account, we have analyzed the radial distribution function (RDF) of water (from the water oxygen atom) around the Zn ion for each tetrapeptide from the full MD simulations in order to elucidate and evaluate possible features pointing into possible inhibition mechanisms. Results are presented in Fig. 5.

The overall results show the existence of a sharp peak for a solvation shell at a medium value of 4.05 Å, suggesting that the water molecules occupy almost all the free-surrounding volume, without being structurally coordinated by the Zn metal atom and thus no considerable interaction between Zn and the water molecules seems to exist, foreclosing the carboxylate-shift equilibrium by excluding solvent access. It resembles the behavior equally observed at the ternary and product complexes [50]. The conclusions drawn at this level are in agreement with other studies, which have pointed out that such aspect could be of particular interest for the design of inhibitors [50]. In addition, we observed that the behavior of different peptides is also characterized by the existence of two additional solvation shells at medium values of 6.35 Å and 8.45 Å, although some are shown to have an additional shell such as CFIM, CVIL and CCIF. In particular, we observe that the peptide CFIM has substantially higher distances of interaction values for both first two shells (6.75 Å and 8.55 Å) than the average values mentioned above. This feature can reveal itself as important because some experimental studies have demonstrated that the highest inhibitory activities seem to be achieved when amino acid residues A1 are nonpolar and aromatic, although a direct implication cannot be done at this level because both low affinity peptides and inhibitors present the same behavior in terms of solvent shells and distance of interaction with the Zn ion.

In addition, the radial distribution function (RDF) of water (from the water oxygen atom) around the cysteine sulfur (S) atom of the CaaX tetrapeptide simulations was also evaluated in order to clarify any possible involvement in the way peptides undergo inhibition. Previous computational studies have confirmed that FPP binds to a hydrophobic cavity of FTase near the metal ion, but without altering the metal coordination sphere [50]. Then, peptide binding proceeds, with the cysteine sulfur atom coordinating the metal coordination sphere in the thiol form and substituting the water molecule in a process where the bidentate form acts as an intermediate [56]. Finally, the Zn-bound peptide thiol substrate loses a proton to an active-site base or to the solvent, resulting in a tightly-bound Zn thiolate and the transfer of the farnesyl moiety from FPP toward the peptide substrate. Accordingly, the solvent around cysteine sulfur proves to be an important trait.

A more heterogeneous perspective was observed with the analysis of RDF results for this particular feature, highlighting the existence of evident differences in the solvation

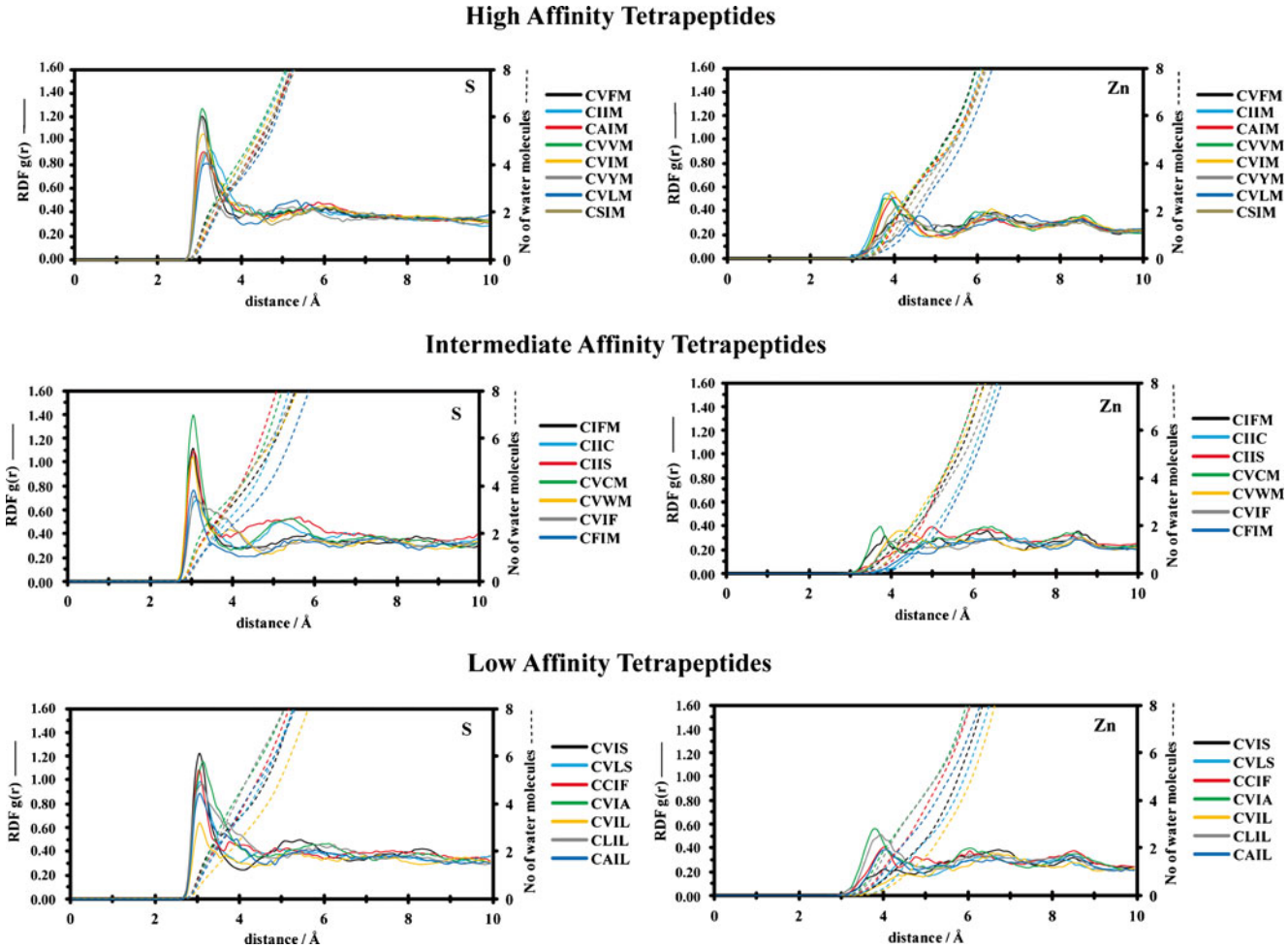

Fig. 5 Radial distribution functions (RDFs,) and cumulative number of water molecules as a function of the distance to the CaaX peptide thiolate sulfur atom (S) and for the active-site Zn atom, calculated for the 22 simulations performed

shells of cysteine sulfur. All peptides yield a sharp peak around 3.05 Å, which indicates a specific interaction between S and the water-oxygen, independently of the FTase possible inhibitory capability of all peptides, which means that this interaction does not seem to be the most relevant aspect concerning inhibition. However, the (non)existence of additional shells can point out a possible inhibitory mechanism of some peptides by excluding water in the vicinity of the cysteine sulfur atom coordinating the metal coordination sphere in the thiol form and thus the equilibrium by carboxylate-shift would be disrupted and the substitution of the water molecule in a process where the bidentate acts as an intermediate would not take place.

A group of peptides namely CAIL, CLIL, CVLS, CVFM, CVYM, CVVM, CIFM, CIIM demonstrate the existence of only one solvation shell and taking into consideration the above, we could possibly include some of these peptides as potential inhibitors. Some modeling studies, together with IC_{50} values derived from experimental studies, have given evidence that some peptides, such as CVFM and CIIM, seem to behave like inhibitors. If we consider the IC_{50} values reported in the literature, we can observe that most of them (excluding CAIL e CLIL) can be regarded as potential inhibitors. On the other hand, some peptides like CVWM, CVIA, CVIL, CIIC, CFIM, present three solvation shells, as shown on Fig. 5, which means that these peptides tend to exclude water in fewer extensions and the water seems to be more structured around cysteine, favoring the substitution of water in the bidentate intermediate. Once again, considering IC_{50} values, we can observe that a less homogeneous panorama can be pointed out from this group; in fact, some peptides, like CVIA and CVIL, are considered to behave like low affinity peptides and the remaining peptides, CIIC, CVWM and CFIM, although behaving like inhibitors can be regarded as presenting lower activity (intermediate affinity peptides) than CVFM or CVYM. Other peptides like CVLM, CVIM, CAIM, CVCM, CCIF, CIIS, CVIF and CSIM present a sharp and a less significant peak at the first and second solvation shells, respectively, with some of the highest distance values S-OH_2 at the second

shell (CVIF, CVIM, and CSIM), which suggest that they can be considered potential inhibitors, which is consistent with solvent exclusion and experimental data.

A more comprehensive analysis of Fig. 5 and all the structural elements considered at this level present a possible relation with the RDF analysis of water around the Zn ion and cysteine sulfur. In fact, we can observe that some peptides assigned as inhibitors, such as CVLM, CVYM, CVWM, CIIC, CIIS, CFIM and CSIM exhibit some of the highest values of the average interaction distance for the first solvation shell for catalytic Zn ion, pointing toward the solvent exclusion. Concomitantly, some of the mentioned peptides like CVLM, CVYM, CIIS, and CIFM were shown to have the same pattern for cysteine sulfur solvation.

Hence, these features indicate an encouraging correlation (with some exceptions), between experimental data and computational results, regarding the inhibitory activity of some peptides and the average interaction distance for the first solvation shell for both catalytic Zn ion and the sulfur cysteine.

Conclusions

In this study, the application of molecular dynamics simulations to a set of 22 CaaX tetrapeptides enabled the observation of a reasonable pattern that highlights several dynamic features on the complexes formed by these tetrapeptides with FTase and FPP, with their affinity and inhibitory ability.

RMSF analysis of the MD simulations performed for these 22 CaaX tetrapetides allowed some important relations for different groups of peptides to be obtained. In particular, a profile of low flexibility together with a high flexibility in some of the helices away from the active center was observed in the studies involving low affinity peptides.

The analysis of distances and the hydrogen bonds between water molecules and FPP have shown that some peptides that are assigned to be potential inhibitors, such as CVFM and CIIM, exhibit a significant number of hydrogen bonds with the pyrophosphate moiety of FPP. This seems to be important since a decrease in flexibility through the establishment of hydrogen bonds would reduce the significant increase in the flexibility of the pyrophosphate moiety of FPP induced by peptide coordination. The head-to-head distance parameter does not prove to be crucial in the definition of potential differences between peptides, although some important aspects could arise for a particular set of peptides, mainly CVFM and CVWM.

In particular, the analysis of hydrogen bonds surrounding the pyrophosphate moiety of the FPP molecule and FTase allowed the observation of three rather different hydrogen bonding patterns. Indeed, for all peptides, there is a substantial number of hydrogen bonds with the highly-conserved amino acid residue Lys164α, though they present a significantly lower percentage of occupancy than the set of the other four residues, namely His248β, Arg291β, Lys294β and Tyr300β. The most important interactions are observed for Arg291β and His248β, nevertheless the second one is only important in intermediate affinity peptides. In particular, it is possible to define a significant pattern for low affinity and high affinity peptides in respect to Arg291β and the main atom residues that establish hydrogen bonds and even individual average percentages of occupancy. The most important of these interactions are established between O2B (low affinity peptides) and O1A (intermediate affinity peptides) of the pyrophosphate and the residue. The O1B and O2B pyrophosphate oxygen atoms are responsible for most of the hydrogen bonds observed for high affinity peptides. The amino acid Tyr300β is not important for most of these tetrapeptides, although there are exceptions like CVIS, in which this residue proves to be of crucial importance, since it is the most important hydrogen bond with a percentage of occupancy of 75.2 %. A significant difference is also observed for the hydrogen bond between water molecules and FPP, in which O2A and O2B are the most important oxygen atoms of the pyrophosphate moiety of FPP for interactions with intermediate affinity peptides and high affinity peptides, respectively and equally important for low affinity peptides.

The study of the radial distribution functions of the water molecules around the Zn ion and cysteine sulfur of CaaX tetrapeptides demonstrated the existence of important differences in the solvation pattern for both cases. We can observe that some peptides assigned as high affinity peptides, like CVLM, CVYM, CVWM, CIIC, CIIS, CFIM and CSIM exhibit some of the highest values of the average interaction distance for the first solvation shell for catalytic Zn ion, foreclosing the carboxylate shift equilibrium like the one described for the resting state (solvent exclusion) and therefore resembling a possible inhibition mechanism [5, 50]. The same is observed for some peptides that behave like inhibitors from the analysis of cysteine sulfur solvation, which provide evidence and is consistent with some computational work that targets the interaction with the Zn catalytic ion to be important to the development of potential inhibitors. Moreover, the study establishes that the RDF function for cysteine sulfur seems to be reasonably reliable with the behavior mentioned for the analysis of Zn ion.

Thus, from the group defined, we were able to establish some important features concerning the aspects that may contribute in higher extension for the behavior of peptides as low affinity peptides or high affinity peptides. Firstly, it is possible to observe that insertion of buried side chains residues at the a_2 position is more critical than the a_1 position for inhibition since it presents lower RMSF values. Moreover, CAIL does not compete for farnesylation and

position a_1 can accept a very large variety of residues and mainly accepts a small chain in low affinity peptides, but the a_2 position is much more restricted to a buried side chain residue for inhibitors. For X, Met is the most common amino acid occupying this position for inhibitors and at a_2 position, Tyr, Phe and Met mainly localized in potential high affinity peptides and concomitantly possible inhibitors.

In the series Ca_1IM, small side chains seem to be better accepted than larger ones at position X since it is possible to observe a potency decrease in CFIM (weak inhibitor). In addition, Leu at position a_1 is favorable in intermediate affinity peptides and the highest inhibitory activities seem to be achieved when a_1 and a_2 are aromatic amino acids. Besides, X position shows the highest stringency and methionine seems to be important for inhibition, since all peptides that form this series present this residue at this site. Although some important aspects can be established and could be of particular interest for drug development efforts, additional computational and experimental works are necessary to consolidate the comprehension of catalytic and inhibition mechanisms of FTase at the atomic level.

Acknowledgments We thank the financial support provided by Fundação para a Ciência e a Tecnologia (FCT) (PTDC/QUI-QUI/103118/2008 and grant no. Pest-C/EQB/LA0006/2011).

References

1. Chen WJ, Andres DA, Goldstein JL, Russell DW, Brown MS (1991) Cell 66:327–334
2. Chen WJ, Andres DA, Goldstein JL, Brown MS (1991) Proc Natl Acad Sci USA 88:11368–11372
3. Reiss Y, Goldstein JL, Seabra MC, Casey PJ, Brown MS (1990) Cell 62:81–88
4. Reiss Y, Seabra MC, Armstrong SA, Slaughter CA, Goldstein JL, Brown MS (1991) J Biol Chem 266:10672–10677
5. Sousa SF, Fernandes PA, Ramos MJ (2005) J Biol Inorg Chem 10:3–10
6. Chen WJ, Moomaw JF, Overton L, Kost TA, Casey PJ (1993) J Biol Chem 268:9675–9680
7. Reiss Y, Brown MS, Goldstein JL (1992) J Biol Chem 267:6403–6408
8. Moores SL, Schaber MD, Mosser SD, Rands E, O'Hara MB, Garsky VM, Marshall MS, Pompliano DL, Gibbs JB (1991) J Biol Chem 266:14603–14610
9. Casey PJ, Seabra MC (1996) J Biol Chem 271:5289–5292
10. Hancock JF, Magee AI, Childs JE, Marshall CJ (1989) Cell 57:1167–1177
11. Jackson JH, Cochrane CG, Bourne JR, Solski PA, Buss JE, Der CJ (1990) Proc Natl Acad Sci USA 87:3042–3046
12. Kato K, Cox AD, Hisaka MM, Graham SM, Buss JE, Der CJ (1992) Proc Natl Acad Sci USA 89:6403–6407
13. Dolence JM, Poulter CD (1995) Proc Natl Acad Sci USA 92:5008–5011
14. Takai Y, Sasaki T, Matozaki T (2001) Physiol Rev 81:153–208
15. Barbacid M (1987) Annu Rev Biochem 56:779–827
16. Bos JL (1989) Cancer Res 49:4682–4689
17. Bos JL, Fearon ER, Hamilton SR, Verlaan-de Vries M, van Boom JH, van der Eb AJ, Vogelstein B (1987) Nature 327:293–297
18. Vogelstein B, Fearon ER, Hamilton AD, Kern SE, Preisinger AC, Leppert M, Nakamura Y, White R, Smits AM, Bos JL (1988) New Engl J Med 319:525–532
19. Wallace A, Koblan KS, Hamilton K, Marquis-Omer DJ, Miller PJ, Mosser SD, Omer CA, Schaber MD, Cortese R, Oliff A, Gibbs JB, Pessi A (1996) J Biol Chem 271:31306
20. Sousa SF, Fernandes PA, Ramos MJ (2008) Curr Med Chem 15:1478–1492
21. Pan J, Yeung SCJ (2005) Cancer Res 65:9109–9112
22. Agrawal AG, Somani RR (2009) Min Rev Med Chem 9:638–652
23. Berndt N, Hamilton AD, Sebti SM (2011) Nat Rev Cancer 11:775–791
24. Tsimberidou AM, Chandhasin C, Kurzrock R (2010) Exp Opin Invest Drugs 19:1569–1580
25. Rao S, Cunningham D, de Gramont A, Scheithauer W, Smakal M, Humblet Y, Kourteva G, Iveson T, Andre T, Dostalova J, Illes A, Belly R, Perez-Ruixo JJ, Park YC, Palmer PA (2004) J Clin Oncol 22:3950–3957
26. Van Cutsem E, van de Velde H, Karasek P, Oettle H, Vervenne WL, Szawlowski A, Schoffski P, Post S, Verslype C, Neumann H, Safran H, Humblet Y, Perez Ruixo J, Ma Y, von Hoff D (2004) J Clin Oncol 22:1430–1438
27. Zhang FL, Kirschmeier P, Carr D, James L, Bond RW, Wang L, Patton R, Windsor WT, Syto R, Zhang R, Bishop WR (1997) J Biol Chem 272:10232–10239
28. Whyte DB, Kirschmeier P, Hockenberry TN, Nunez-Oliva I, James L, Catino JJ, Bishop WR, Pai JK (1997) J Biol Chem 272:14459–14464
29. Rowell CA, Kowalczyk JJ, Lewis MD, Garcia AM (1997) J Biol Chem 272:14093–14097
30. Tucker TJ, Abrams MT, Buser CA, Davide JP, Ellis-Hutchings M, Fernandes C, Gibbs JB, Graham SL, Hartman GD, Huber HE, Liu D, Lobell RB, Lumma WC, Robinson RG, Sisko JT, Smith AM (2002) Bioorg Med Chem Lett 12:2027–2030
31. Moorthy NSHN, Sousa SF, Ramos MJ, Fernandes PA (2011) J Enzyme Inhib Med Chem 26:777–791
32. Moorthy NSHN, Sousa SF, Ramos MJ, Fernandes PA (2011) J Biomol Screen 16:1037–1046
33. Perez MAS, Sousa SF, Oliveira EFT, Fernandes PA, Ramos MJ (2011) J Phys Chem B 115:15339–15354
34. Long SB, Casey PJ, Beese LS (2000) Struct Fold Des 8:209–222
35. Reid TS, Terry KL, Casey PJ, Beese LS (2004) J Mol Biol 343:417–433
36. Long SB, Hancock PJ, Kral AM, Hellinga HW, Beese LS (2001) Proc Natl Acad Sci USA 98:12948–12953
37. Sousa SF, Fernandes PA, Ramos MJ (2005) Biophys J 88:483–494
38. Sousa SF, Fernandes PA, Ramos MJ (2007) J Comput Chem 28:1160–1168
39. Tamames B, Sousa SF, Tamames J, Fernandes PA, Ramos MJ (2007) Proteins 69:466–475
40. Park HW, Boduluri SR, Moomaw JF, Casey PJ, Beese LS (1997) Science 275:1800–1804
41. Long SB, Casey PJ, Beese LS (2002) Nature 419:645–650
42. Tobin DA, Pickett JS, Hartman HL, Fierke CA, Penner-Hahn JE (2003) J Am Chem Soc 125:9962–9969
43. Pickett JS, Bowers KE, Fierke CA (2003) J Biol Chem 278:51243–51250
44. Bowers KE, Fierke CA (2004) Biochemistry 43:5256–5265
45. Pickett JS, Bowers KE, Hartman HL, Fu HW, Embry AC, Casey PJ, Fierke CA (2003) Biochemistry 42:9741–9748
46. Hartman HL, Bowers KE, Fierke CA (2004) J Biol Chem 279:30546–30553
47. Ho MH, De Vivo M, Dal Peraro M, Klein ML (2009) J Chem Theor Comput 5:1657–1666

48. Cui G, Merz KM (2007) Biochemistry 46:12375–12381
49. Sousa SF, Fernandes PA, Ramos MJ (2007) Theor Chem Acc 117:171–181
50. Sousa SF, Fernandes PA, Ramos MJ (2009) Bioorg Med Chem 17:3369–3378
51. Sousa SF, Fernandes PA, Ramos MJ (2008) Int J Quant Chem 108:1939–1950
52. Sousa SF, Fernandes PA, Ramos MJ (2008) J Phys Chem B 112:8681–8691
53. Sousa SF, Fernandes PA, Ramos MJ (2007) Proteins 66:205–218
54. Mirza UA, Chen GD, Liu YH, Doll RJ, Girijavallabhan VM, Ganguly AK, Pramanik BN (2008) J Mass Spectrom 43:1393–1401
55. Sousa SF, Fernandes PA, Ramos MJ (2005) J Mol Struct (THEOCHEM) 729:125–129
56. Sousa SF, Fernandes PA, Ramos MJ (2009) Chemistry 15:4243–4247
57. Sousa SF, Fernandes PA, Ramos MJ (2007) J Am Chem Soc 129:1378–1385
58. Rardin RL, Tolman WB, Lippard SJ (1991) New J Chem 15:417–430
59. Goldstein JL, Brown MS, Stradley SJ, Reiss Y, Gierasch LM (1991) J Biol Chem 266:15575–15578
60. Reiss Y, Stradley SJ, Gierasch LM, Brown MS, Goldstein JL (1991) Proc Natl Acad Sci USA 88:732–736